

# UC Irvine

## UC Irvine Previously Published Works

### Title

The Influence of Mallet Mass and Velocity on the Fracture Patterns in Osteotomies

### Permalink

<https://escholarship.org/uc/item/8m0923s4>

### Journal

The Laryngoscope, 135(1)

### ISSN

0023-852X

### Authors

Goshtasbi, Khodayar

Kim, Daniel

Torabi, Sina J

et al.

### Publication Date

2025

### DOI



10.1002/lary.31647

### Copyright Information

This work is made available under the terms of a Creative Commons Attribution License, available at <https://creativecommons.org/licenses/by/4.0/>

Peer reviewed

# The Influence of Mallet Mass and Velocity on the Fracture Patterns in Osteotomies

Khodayar Goshtasbi, MD ; Daniel Kim, BA; Sina J. Torabi, MD; Theodore V. Nguyen, MD   
Brigitte A. Chung; Ellen M. Hong, BS; John Vu, BS; Jessica Salas, PhD; Justin S. Kim;  
Brian J.F. Wong, MD PhD

**Introduction:** Osteotomies are routinely incorporated in rhinoplasty, however, the influence of mass, velocity, kinetic energy (KE), and momentum ( $p$ ) of the mallet on fracture patterns has not been studied.

**Methods:** An experimental sledge guillotine setup was designed simulating a mallet strike with adjustable height and mass and 2 mm-thick Sawbone blocks. KE and  $p$  were calculated using  $KE = \frac{1}{2} \text{ mass} \times \text{velocity}^2$  and  $p = \text{mass} \times \text{velocity}$  formulas. Fracture lengths and angles were measured.

**Results:** Ten groups with varying mallet masses and drop heights were tested with 10 bones per group. Fracture length positively correlated with KE ( $R = 0.542$ ,  $p < 0.001$ ) and  $p$  ( $R = 0.508$ ,  $p < 0.001$ ). Fracture angle also positively correlated with KE ( $R = 0.367$ ,  $p < 0.001$ ) and  $p$  ( $R = 0.329$ ,  $p < 0.001$ ). In groups with similar KE, osteotomies with higher  $p$  (heavier mallet with slower velocity) had greater fracture lengths ( $29.31 \pm 0.68$  vs.  $27.68 \pm 2.12$  mm,  $p = 0.013$ ) but similar fracture angles ( $p = 0.189$ ). In groups with similar  $p$ , osteotomies with higher KE (lighter hammer with faster velocity) had significantly greater fracture lengths ( $28.28 \pm 1.28$  vs.  $20.45 \pm 12.20$  mm,  $p = 0.041$ ) and greater divergent fracture angles ( $3.13 \pm 1.97^\circ$  vs.  $1.40 \pm 1.36^\circ$ ,  $p = 0.031$ ). Regression modeling of the relationship between KE and fracture lengths and angles demonstrated that cubic followed by logarithmic regression models had the best fits.

**Conclusion:** Osteotomy fracture patterns positively correlated with the mallet's KE more so than its  $p$ , suggesting that the mallet's velocity has an increased impact effect than its mass. Clinically, a heavier mallet with a lower velocity will likely generate a smaller fracture length and fracture angle, indicating a more controlled and ideal fracture.

**Key Words:** fracture patterns, kinetic energy, momentum, osteotome, osteotomy, rhinoplasty.

**Level of Evidence:** NA

*Laryngoscope*, 135:97–103, 2025

## INTRODUCTION

Depending on the type of nasal deformity, rhinoplasty surgeries routinely involve lateral, medial, or transverse osteotomies. When performed inappropriately, osteotomies can lead to soft tissue damage, edema, aesthetic deformities, and other complications.<sup>1,2</sup> Previous studies have investigated the effect of osteotome type, osteotome sharpness, and applied force on the fracture patterns in an effort to improve the safety and efficiency of osteotomies.<sup>3–6</sup> In addition, there are also studies investigating the efficacy of piezosurgery on percutaneous osteotomies.<sup>7,8</sup> However, a critical aspect, namely the

kinetic energy (KE) and momentum ( $p$ ) of the mallet, has received limited attention regarding its influence on fracture patterns. During an osteotomy, the osteotome is repeatedly hit with a mallet whose mass and geometry is selected by the surgeon. The strike terminal velocity is determined by the rate of the mallet acceleration controlled by the surgeon and the change in height during the process. The mass and velocity of the mallet at the time of impact then affects the kinetic energy ( $KE = \frac{1}{2} \text{ mass} \times \text{velocity}^2$ ) and momentum ( $p = \text{mass} \times \text{velocity}$ ) transferred to the osteotome. Variations in KE and  $p$  are significant and can influence the interaction of the osteotome with the bone and the resultant fracture pattern. It is known that focused application of inertial force within a narrow impact zone yields the highest efficacy in force transfer. Although a study by Lee et al. suggested that applying lower acceleration can lead to more unpredictable fracture patterns,<sup>5</sup> there was no quantitative analysis and no information on whether mass or velocity—or KE and  $p$ —have a greater impact on the resulting fracture patterns.

When analyzing bony fracture patterns caused by the osteotome and mallet, there are two crucial metrics: fracture length and divergent fracture angle. Fracture length is the length of the fracture in the bone from the point of contact with the osteotome—differing fracture

From the Department of Otolaryngology-Head and Neck Surgery (K.G., S.J.T., T.V.N., B.J.F.W.), University of California Irvine, Irvine, California, U.S.A.; Beckman Laser Institute (K.G., D.K., S.J.T., T.V.N., B.A.C., E.M.H., J.V., J.S., J.S.K., B.J.F.W.), University of California Irvine, Irvine, California, U.S.A.; and the School of Biomedical Engineering (B.J.F.W.), University of California Irvine, Irvine, California, U.S.A.

Editor's Note: This Manuscript was accepted for publication on July 01, 2024.

The authors have no funding, financial relationships, or conflicts of interest to disclose.

Portions of this work have been accepted as a podium presentation at the Triological Society Combined Sections Meeting, January 25–27, 2024, West Palm Beach, FL.

Send correspondence to Brian J.F. Wong, Department of Otolaryngology – Head and Neck Surgery, University of California, Irvine 1002 Health Sciences Road Irvine, CA 9261; Email: [bjwong@uci.edu](mailto:bjwong@uci.edu)

DOI: 10.1002/lary.31647

lengths are optimal depending on the context, though, generally, a shorter length gives the surgeon more control. On the other hand, fracture angle is the angle at which the fracture deviates from center line defined by the trajectory of the osteotome along its axis. The angle is between this pathway and the actual fracture line created during mallet strikes. Generally, smaller fracture angles are desirable because they indicate a more controlled and predictable break in line with osteotome trajectory.

This is the first study that systematically explores the effect of mallet mass and velocity (KE and  $p$ ) on the length and angular deviation of osteotomy fractures using synthetic bone phantoms. Secondly, this study aims to determine what combination of mallet weight and impact velocity (e.g., hitting an osteotome with a heavy hammer with a slower velocity vs. a heavy hammer from with a faster velocity) may have a more pronounced effect on the fracture patterns.

## METHODS

The osteotomy simulation system was constructed onto a  $26 \times 13$ -inch wooden platform (Figure 1). All wood components were cut to size within a hundredth of an inch with a table saw, and the assembly was secured with nails and screws. Dimensions

of the apparatus were validated and verified in SOLIDWORKS (Waltham, MA) through vibration and physical dynamics analysis tools. The setup, reminiscent of a guillotine's mechanical characteristics, consisted of two sturdy vertical posts positioned 4 inches apart, each measuring  $1.5 \times 2.5 \times 23.75$  inches. To ensure their upright stability and alignment, two steel angle corner brackets, specifically the MP9221 prime-line hole brackets, were affixed lengthwise against the posts, securely fastening them to the  $26 \times 13$  platform. Additionally, two broader strong-tie angle brackets were placed widthwise against the posts to minimize the potential for shifting and vibration during experiments. A tubular spirit level and a right triangle were employed throughout the assembly process to guarantee precise alignment. On the inner sides of the posts, drawer slides with ball bearing side mount glides were installed on the inner sides of the posts, positioning them 10.5 inches from the base where the posts met the platform. The dropping block or sledge, responsible for descending and striking the osteotome, measured  $3 \times 1.25 \times 2.25$  inches. Regular greasing was conducted at four-month intervals to ensure minimal friction and smooth operation of the rail system. The 3D printing process was conducted on a Formlabs (Somerville, MA) 3D printer, the Form 2 model, utilizing Clear v4 resin. Within this process, all 3D printed components, including the flag responsible for passing through the photogate to record precise data on the descending block's velocity, as well as the osteotome material holder designed to constrain movement along the  $x$ ,  $y$ , and  $z$  axes, were meticulously designed and

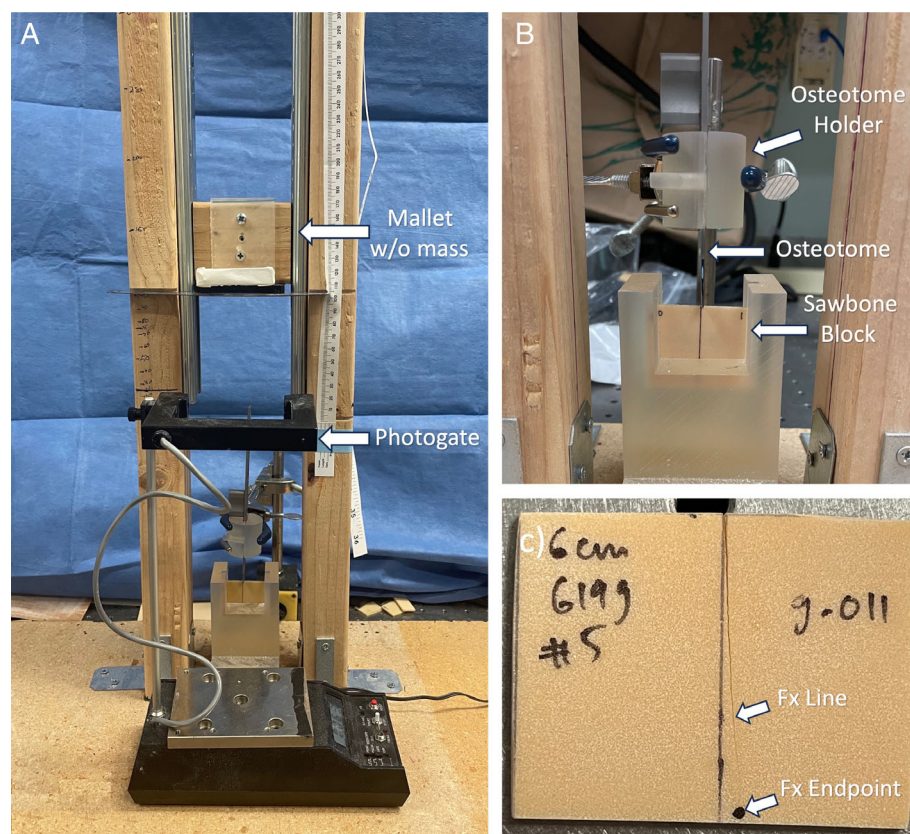


Fig. 1. The experimental setup. (A) Demonstrates the overall setup where the top wooden block is acting as a mallet. The mallet's weight can be increased with screwing additional metallic weights to it, and its release height can be adjusted according to the sideline ruler. It also shows the photogate which measures the velocity of the osteotome at the time of impact. (B) Shows a close-up of the osteotome setup where an osteotome holder keeps the osteotome stationary at a vertical angle, where it will hit the sawbone blocks at midline after mallet is released. (C) Shows an example of a Sawbone block after impact (experiment #5, 619 mallet weight released at 6 cm) where fracture line and fracture endpoint are demonstrated.

subsequently produced using SolidWorks computer aided design (CAD) software and 3D printing technology. Velocity of the hammer at the time of impact was measured using a photogate, by calculating distance/time. The photogate setup incorporated a Pasco ME-9215A Photogate Timer with Memory and a Photogate 9215. The photogate was positioned 2 inches away the posts, thus enabling calculation of the descent speed of the falling block during experiments. KE and  $p$  were calculated using the  $KE = \frac{1}{2} \text{mass} \times \text{velocity}^2$  and  $p = \text{mass} \times \text{velocity}$  formulas. SawBones (Vashon Island, WA) are porous polymer phantoms that emulate bones and are widely used for didactic purposes among surgical specialties. These were precisely cut to  $40 \times 30$  mm size and 2 mm thickness, and meant to simulate real-life bone tissue. A midline vertical pencil line at 20 cm was drawn to indicate the osteotomy impact position.

Ten different groups with different mallet drop heights and masses were examined. The baseline mass of the mallet was 223 g. In group 1–4, the mallet was dropped from 3 cm with fluctuating masses, corresponding to 223 g in group 1 (baseline mass), 325 g in group 2 (102 g added mass), 473 g in group 3 (250 g added mass), and 842 g in group 4 (619 g added mass). In group 5–8, the mallet was dropped from 6 cm with varying mass, corresponding to 223 g in group 5, 325 g in group 6, 473 g in group 7, and 842 g in group 8. In groups 9 and 10, the mallet with no additional mass (223 g) was dropped from 9 and 12 cm heights, respectively. Ten SawBones for each of the 10 groups were used. The osteotome was sharpened before each hit, via the most efficient sharpening method as described in a previous article.<sup>6</sup> When the bone did not fracture, it was recorded as 0 for fracture length/angle and hit again. For each bone, the end of the fracture line was marked, which would be compared to the drawn midline mark. The fracture line would then be analyzed in respect to its length (distance from point of impact) and angle (deviation from midline). In an ideal world, the osteotome would have a perpendicular impact on the edge of the specimen and then transverse the specimen in a predictable length and without deviation from midline. In practice, the fracture length and angle vary. The variation can be due to the inhomogeneity of the bone leading to preferential propagation of the fracture off axis. It is also possible that as one “hits” the mallet at a slightly faster acceleration, the osteotome may be struck off axis, whereas a “lighter” strike may be more precise. We expect the guillotine system in this experiment to provide a more controlled experimental setting than a free-weight osteotomy scenario and thus control for other confounders (e.g., angles, variable forces) while evaluating the effect of kinetic energy and momentum.

Photographs of the broken SawBones were uploaded to ImageJ (open source software, version 1.53 t). Image calibration was performed by designating the left-sided bone height as 30 mm. Next, the fracture length (in mm) and fracture angle (in degrees, compared to the midline vertical line) were measured via ImageJ. Statistical analyses were performed via PASW Statistics 18.0 software (SPSS Inc., Chicago, Illinois). A  $p$ -value threshold of  $<0.05$  was designated for statistical significance. When continuous variables (e.g., KE,  $p$ , fracture angle, fracture length) were compared between more than two groups via ANOVA analysis, post hoc LSD (least significant difference) analysis was used to compare groups individually with each other. Lastly, the scattered plot data of KE versus fracture length, and KE versus fracture angle, were mathematically modeled for linear/nonlinear curves of best fit, and R values were used to compare the comparative acceptability of the models.

## RESULTS

Ten bones for each of the 10 groups were used. Table I summarizes the distance and mass of each run as well as the calculated velocity, KE, and  $p$ . As expected, there was a significant positive correlation between KE and  $p$  (Pearson Correlation coefficient  $R = 0.919$ ,  $p < 0.001$ ). Furthermore, there was a significant positive correlation between drop height and velocity ( $R = 0.979$ ,  $p < 0.001$ ), as expected.

Table I also summarizes the average fracture length and fracture angles resulting from osteotomy strikes in each group. Overall, there was a positive correlation between fracture length and fracture angle ( $R = 0.598$ ,  $p < 0.001$ ). Fracture length was positively correlated with both KE ( $R = 0.542$ ,  $p < 0.001$ ) and  $p$  ( $R = 0.508$ ,  $p < 0.001$ ). Fracture angle was also positively correlated with both KE ( $R = 0.367$ ,  $p < 0.001$ ) and  $p$  ( $R = 0.329$ ,  $p < 0.001$ ). Furthermore, compared to  $p$ , KE had a slightly greater Pearson Correlation with both fracture length and fracture angle. Figure 2 shows the relationship between KE or  $p$  as independent variables and fracture length or fracture angle as dependent variables.

Of note, strikes resulting in no fracture creation were prevalent in group 1 ( $N = 10$ ), group 2 ( $N = 10$ ), group 3 ( $N = 3$ ), and group 5 ( $N = 3$ ) which contribute to

TABLE I.

Summary of the 10 Experimental Groups With the Measured Momentum, Kinetic Energy, and the Resultant Osteotomy Fracture Length and Fracture Angles. The Baseline Mass of the Mallet was 223 g, Corresponding to Groups 1, 5, 9, and 10 Where no Additional Masses Were Added.

Group	Mallet distance, total mass	Velocity	Momentum ( $p$ )	Kinetic energy (KE)	Fracture length (mm)	Fracture angle (deg)
1	3 cm, 223 g	$1.12 \pm 0.07$	$0.25 \pm 0.02$	$0.14 \pm 0.02$	$6.46 \pm 10.75$	$0.59 \pm 1.36$
2	3 cm, 325 g	$1.11 \pm 0.02$	$0.36 \pm 0.01$	$0.20 \pm 0.01$	$11.53 \pm 13.07$	$1.25 \pm 1.77$
3	3 cm, 473 g	$1.18 \pm 0.03$	$0.56 \pm 0.01$	$0.33 \pm 0.02$	$20.45 \pm 12.20$	$1.40 \pm 1.36$
4	3 cm, 842 g	$1.22 \pm 0.04$	$1.03 \pm 0.03$	$0.63 \pm 0.04$	$29.31 \pm 0.67$	$3.05 \pm 2.30$
5	6 cm, 223 g	$1.92 \pm 0.05$	$0.43 \pm 0.01$	$0.41 \pm 0.02$	$20.25 \pm 10.66$	$1.67 \pm 1.48$
6	6 cm, 325 g	$1.98 \pm 0.05$	$0.65 \pm 0.02$	$0.64 \pm 0.03$	$27.68 \pm 2.12$	$2.29 \pm 1.67$
7	6 cm, 473 g	$2.00 \pm 0.01$	$0.95 \pm 0.01$	$0.95 \pm 0.01$	$28.91 \pm 0.80$	$1.74 \pm 1.40$
8	6 cm, 842 g	$2.09 \pm 0.11$	$1.76 \pm 0.09$	$1.84 \pm 0.20$	$29.61 \pm 0.85$	$3.19 \pm 1.95$
9	9 cm, 223 g	$2.50 \pm 0.01$	$0.56 \pm 0.01$	$0.70 \pm 0.01$	$28.24 \pm 1.28$	$3.13 \pm 1.97$
10	12 cm, 223 g	$3.04 \pm 0.17$	$0.68 \pm 0.04$	$1.03 \pm 0.12$	$29.35 \pm 0.53$	$3.16 \pm 2.53$



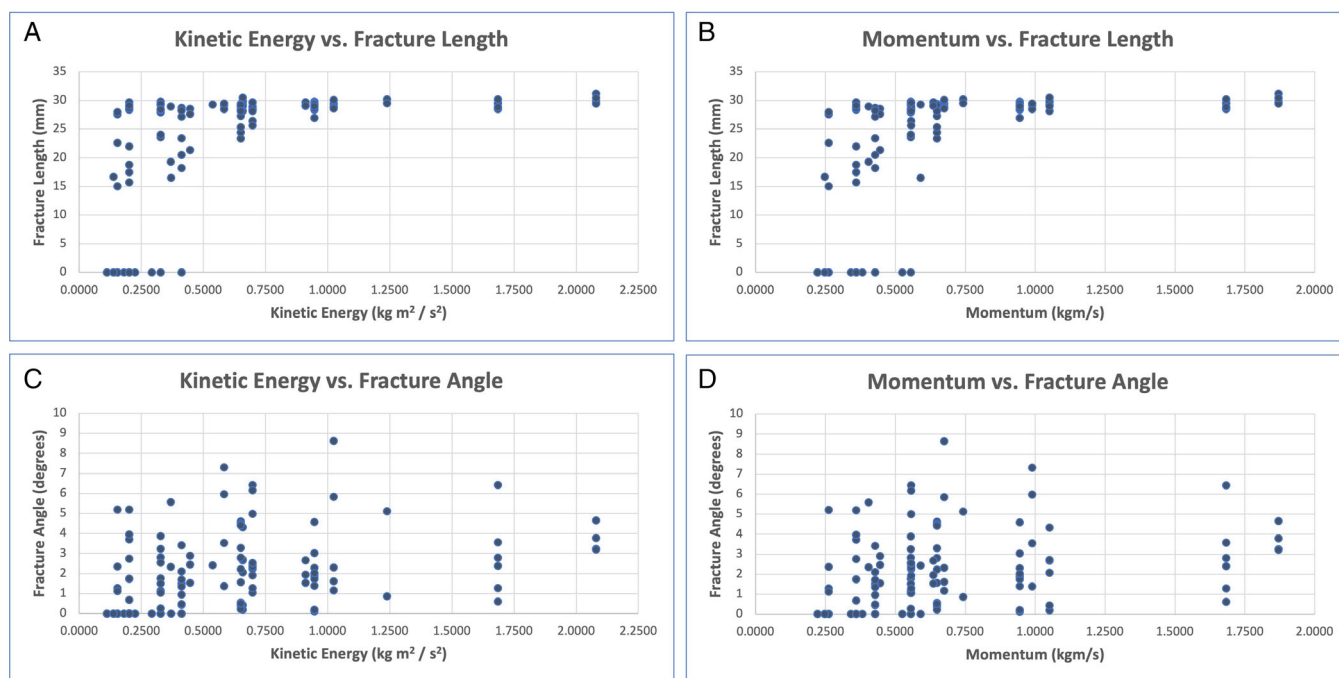


Fig. 2. Relationship between kinetic energy (A and C) or momentum (B and D) as independent variables with fracture length (A and B) or fracture angle (C and D) as dependent variables.

the inflated standard deviation values. Only group 1 had instances of needing more than two strikes (range 3–4) to initiate a fracture (in four instances). If the non-breaking strikes were removed, KE remained positively correlated with fracture length ( $R = 0.450$ ,  $p < 0.001$ ) but not with fracture angle ( $R = 0.137$ ,  $p = 0.179$ ).

Groups 1–4 had increasing mass in the setting of constant 3 cm drop height (and thus, relatively similar terminal velocities), which corresponded to an increase in  $p$  and KE as expected. One-way ANOVA showed that the four groups had significantly different fracture lengths ( $p < 0.001$ ) and fracture angles ( $p = 0.006$ ). Table I demonstrates that as KE and  $p$  increase from group 1 to 4, fracture length and fracture angle increase accordingly.

Group 5–8 similarly had increasing mass in the setting of constant drop from a higher distance of 6 cm, which corresponded to an increase in velocity,  $p$ , and KE as expected. One-way ANOVA showed a statistical difference between the fracture lengths ( $p = 0.002$ ) although post hoc analysis showed that the difference only existed between group 5 and the rest of the groups (group 5 being significantly lower), while groups 6–8 had similar fracture lengths to each other. On one-way ANOVA, group 5–8's difference in fracture angles did not meet statistical significance ( $p = 0.092$ ).

Groups 1, 5, and 9–10 had increasing drop height (and resultant increasing velocities) in the setting of constant mass, which corresponded to an increase in velocity,  $p$ , and KE as expected. One-way ANOVA showed a statistical difference between the fracture lengths ( $p < 0.001$ ) and post hoc analysis showed statistical difference between all groups except between group 9 and

10, suggesting a significant increase initially but plateauing after 9 cm. There was also a statistical difference in fracture angle between the groups ( $p < 0.001$ ) where post hoc analysis shows difference between all values except between groups 1 and 5 and between 9 and 10, suggesting a significant increase after a threshold beyond 6 cm.

Groups with similar KE but different  $p$ , and vice versa, can be compared as follows. Group 4 (3 cm, 619 g) and 6 (6 cm, 102 g) had statistically similar KE ( $p = 0.662$ ) but different  $p$ . Compared to group 6, group 4 with the higher  $p$  had significantly greater fracture lengths ( $27.68 \pm 2.12$  vs.  $29.31 \pm 0.68$ ,  $p = 0.013$ ) while fracture angles were statistically similar ( $p = 0.189$ ). On the other hand, group 3 (3 cm, 250 g) and 9 (9 cm, no additional mass) had statistically similar  $p$  ( $p = 0.854$ ) but different KE. Compared to group 3, group 9 with the higher KE had significantly higher fracture lengths ( $28.28 \pm 1.28$  vs.  $20.45 \pm 12.20$ ,  $p = 0.041$ , larger difference than the aforementioned example) and fracture angles ( $3.13 \pm 1.97$  vs.  $4.40 \pm 1.36$ ,  $p = 0.031$ , significant unlike the aforementioned example).

Lastly, statistical analysis on the relationship between KE and fracture length or fracture angle (scattered data from Fig. 1) using different models (linear, logarithmic, and cubic curved fits) was attempted, and the results are shown in Figure 3 for fracture length and Figure 4 for fracture angle, with the former having better correlation coefficients. The cubic regression models followed by logarithmic and then linear models had the best fit (largest R value) in both scenarios.

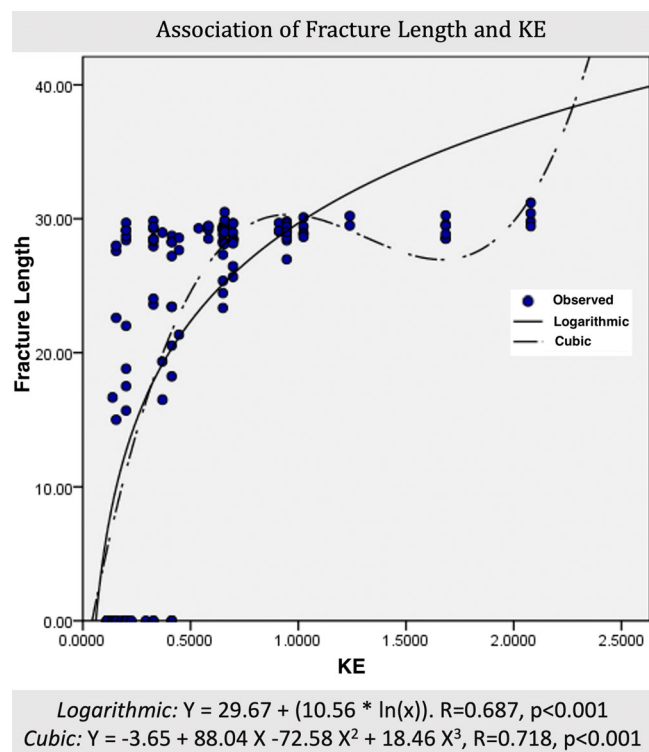


Fig. 3. Mathematical modeling of the relationship between kinetic energy and fracture length.

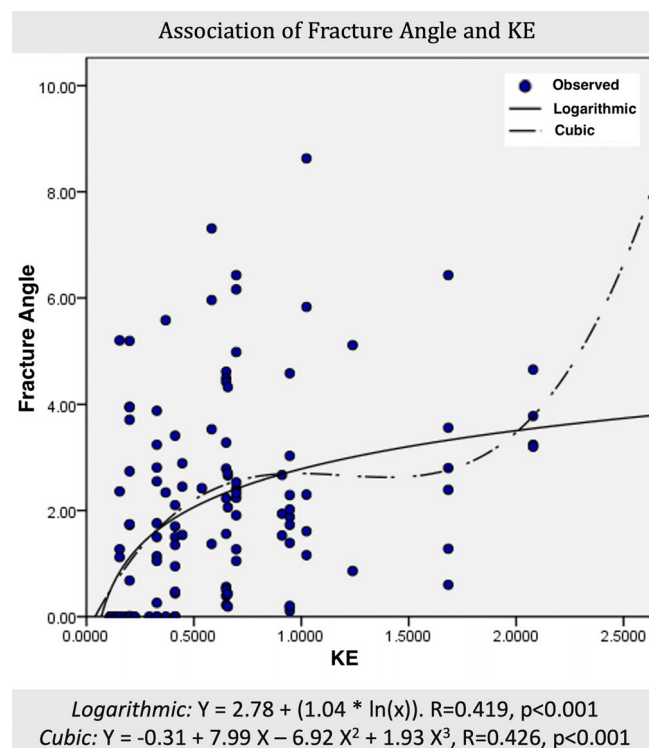


Fig. 4. Mathematical modeling of the relationship between kinetic energy and fracture angle.

## DISCUSSION

Prior osteotomy studies have focused specifically on the sharpness of osteotomes and the type of osteotomes used to generate more favorable and predictable fracture patterns.<sup>5,6</sup> Even the studies on piezosurgery are limited on their scope of osteotomy variability and predictability.<sup>7,8</sup> Previous studies in the literature have not focused on how the mass and velocity of the osteotome mallet may quantitatively impact the resulting fracture patterns. Different phantom models that incorporate osteotomy applications have been introduced in the fields of orthopedic and orthognathic surgery.<sup>9-12</sup> However, this is the first study to incorporate a novel and somewhat homogeneous phantom osteotomy model resembling human nasal bone, and quantitatively analyze the influence of mallet mass and drop distance, and thus the velocity, KE, and  $p$ , on bony fracture patterns, interpreted via an analysis of fracture length and angle. Mass and velocity of the mallet (and hence, KE and  $p$ ) positively correlate with the fracture lengths and fracture angles, with a plateau effect for drop heights above 6 cm or a mass greater than 102 g, above which fracture length and angle did not vary drastically. The results of this study also indicate that kinetic energy played a more significant role in determining fracture length and angle than momentum. When comparing the two groups with similar KE (groups 4 and 6), the group with the greater  $p$  caused longer fracture length but a statistically similar fracture angle. This can be explained by the property of momentum, which can be thought of as the change in force over the change in time required to bring an object from its initial velocity to rest. In this case, it would require more force to stop an object with the higher  $p$ , which explains why when both groups had similar KE, the group with the greater mass and therefore greater  $p$  caused a longer fracture length. On the other hand, while comparing the two groups with similar  $p$  (groups 3 and 9), the group with the higher KE caused a significantly longer fracture length and larger fracture angle. The difference in fracture lengths was more pronounced than in the previous case where two groups of similar KE were compared, and furthermore, there was a significant difference with fracture angle (higher KE leading to higher and thus worst fracture angle). These imply that KE, rather than  $p$ , is the better predictor of nonideal fracture patterns. This is further supported by the finding that compared to  $p$ , KE had a slightly larger correlation with both fracture length and fracture angle. These results also suggest that the velocity (derived from drop height) has a greater impact on the resulting fracture pattern than the mass of the mallet. Since the KE of the mallet is linearly related to the mass of the mallet and quadratically related to the velocity of the mallet, and given that KE is a better predictor of fracture patterns than momentum, the velocity (and thus, drop height) is a better predictor of a nonideal fracture pattern than the mallet's mass.

Momentum and kinetic energy are related yet distinct physical concepts and are associated with different conservation laws. The momentum of an object can be

conceptualized as the amount of force that must be applied to stop an object over a given time. On the other hand, the kinetic energy of an object can be interpreted as the amount of force necessary to stop an object over a given distance. Though a greater kinetic energy necessarily implies a greater momentum and vice versa, our results suggest that kinetic energy, not momentum, is the better predictor for fracture lengths and divergent fracture angles. The reasoning behind this is apparent when considering that it is the application of the force of the osteotome over a particular distance that causes the fracture to propagate. The correlation between kinetic energy and “damage” has been known since the experimental verification of the formula for kinetic energy in the 18th century, when Wilhelm Jacob’s Gravesande dropped balls onto clay and found that the depth of the indentation was proportional to the square of the velocity.<sup>13</sup> A recent study in marine engineering further verifies this observation; according to Ye et al., kinetic energy is a better measure than momentum for quantifying the impact of vessels.<sup>14</sup> Regardless, the literature on fracture generation and propagation is complex, and nearly absent in the context of bone tissue, let alone facial bones.

This brings us to the theoretical question of whether a heavier mallet with a slower velocity or a smaller mallet with a larger velocity will generate a more optimal fracture. This study suggests that a larger/heavier mallet dropped at a shorter distance with a lower velocity will likely have a smaller KE and therefore generate a smaller fracture length and less divergent, off-axis fracture angle (indicating a more controlled and ideal fracture) than a smaller/lighter mallet dropped at a longer distance with a higher velocity. Furthermore, even when comparing a “heavy hammer with low velocity” and “light hammer with high velocity” such that KE is similar, our results indicate that in this scenario also, the “heavy hammer with low velocity” may yield more predictable outcomes in a clinical context. Comparing Group 4 (3 cm, 619 g) and 6 (6 cm, 102 g) with similar KE showed that the “heavy hammer with slower velocity” (Group 4) resulted in greater fracture lengths (with smaller standard deviations) and similarly larger divergent fracture angles, when the height difference was about 3 cm. Therefore in a clinical setting, heavier mallets with controlled speeds of impact will likely achieve more straighter osteotomies (more predictable fracture length and lower deviation from midline) than smaller hammers with greater velocity at impact.

The findings of this study should be interpreted in the context of its limitations. First, although this experiment utilized a phantom model to establish a controlled experimental setting, the SawBones are far from exact proxies for human nasal bones; these are porous polymer massed structures that are largely homogenous. Just like the human nasal bone, the SawBones are an inhomogeneous material, porous with texture, but not periodic fine structure. It is also difficult to precisely machine these specimens into precise geometric properties and sizes which can theoretically introduce some inconsistency in the experiment. Regardless, we believe that the presented phantom SawBone model is of close proximity to

represent human nasal bone fractures in response to osteotomy trials. Second, this study did not compare different osteotome types and thus the results may not directly extrapolate to all types of osteotomes. Furthermore, given that this experiment did not use a human model, a variety of outcomes such as soft tissue injury, edema, etc. could not be measured, which are nevertheless important factors in the setting of rhinoplasty. Another limitation is that our osteotome was guided using a rail system with friction. This friction may have impact on results, though we used a photogate to estimate terminal velocity before the strike. Lastly, in real clinical circumstances, the assistant’s mallet strikes can vary from tap to tap in regard to terminal velocity, angle of impact, and trajectory, while the velocity and point/angle of impact were controlled to the best of our ability in this experiment. Ideally, an osteotome traverses bony tissue along a user defined pathway, and this study also suggests that increasing the velocity can make the propagation lengthier and off angle, leading to a less ideal osteotomy. Despite the aforementioned limitations, the study offers novel information on the osteotomy fracture patterns depending on the mallet mass, velocity, and the kinetic energy and momentum at the impact, which may be of value to the surgeon performing osteotomies through thin bone or in purchasing a mallet.

## CONCLUSION

During osteotomies, the kinetic energy and momentum of the mallet were positively correlated with the bony fracture lengths and divergent fracture angles. Fracture patterns correlated more positively with kinetic energy than momentum, suggesting that mallet’s velocity has a greater impact on the resulting fracture pattern than its mass. In our experiment, drop heights larger than 6 cm and masses larger than 102 g led to a plateauing effect with no further significant changes in fracture patterns. In a clinical setting, a heavier mallet with a lower velocity will likely have a smaller KE and therefore generate a smaller fracture length and divergent fracture angle (indicating a more controlled and ideal fracture) than a lighter mallet with a higher velocity.

## BIBLIOGRAPHY

1. Giacomarra V, Russolo M, Arnez ZM, Tirelli G. External osteotomy in rhinoplasty. *Laryngoscope*. 2001;111(3):433-438.
2. Gruber RP. Aesthetic and technical aspects of nasal osteotomies. *Oper Tech Plast Reconstr Surg*. 1995;2(1):2-15.
3. Gabra N, Rahal A, Ahmarani C. Nasal osteotomies: a cadaveric study of fracture lines. *JAMA Facial Plast Surg*. 2014;16(4):268-271.
4. Kuran I, Ozcan H, Usta A, Bas L. Comparison of four different types of osteotomes for lateral osteotomy: a cadaver study. *Aesthet Plast Surg*. 1996;20(4):323-326.
5. Lee HM, Kang HJ, Choi JH, Chae SW, Lee SH, Hwang SJ. Rationale for osteotome selection in rhinoplasty. *J Laryngol Otol*. 2002;116(12):1005-1008.
6. Nguyen TV, Park AC, Hernandez K, et al. Developing the optimal osteotome hand-sharpening method. *Facial Plast Surg Aesth Med*. 2023;25(4):318-324.
7. Robiony M, Lazzarotto A, Nocini R, Costa F, Sembroni S, Franz L. Piezosurgery: ten years’ experience of percutaneous osteotomies in rhinoplasty. *J Oral Maxillofac Surg*. 2019;77(6):1237-1244.
8. Kisel J, Khatib M, Cavale N. A comparison between Piezosurgery and conventional osteotomies in rhinoplasty on post-operative Oedema and ecchymosis: a systematic review. *Aesthet Plast Surg*. 2023;47(3):1144-1154.

9. Gebhardt C, Götting L, Buchberger L, et al. Femur reconstruction in 3D ultrasound for orthopedic surgery planning. *Int J Comput Assist Radiol Surg.* 2023;18(6):1001-1008. <https://doi.org/10.1007/s11548-023-02868-4> Epub 2023 Apr 20.
10. Papachristou G. Photoelastic study of the internal and contact stresses on the knee joint before and after osteotomy. *Arch Orthop Trauma Surg.* 2004; 124(5):288-297. <https://doi.org/10.1007/s00402-004-0657-6> Epub 2004 Apr 2.
11. Han JJ, Woo SY, Yi WJ, Hwang SJ. Robot-assisted maxillary positioning in orthognathic surgery: a feasibility and accuracy evaluation. *J Clin Med.* 2021;10(12):2596.
12. Gui H, Zhang S, Luan N, Lin Y, Shen SG, Bautista JS. A novel system for navigation-and robot-assisted craniofacial surgery: establishment of the principle prototype. *J Craniofac Surg.* 2015;26(8):e746-e749.
13. Bernoulli, Daniel. *Hydrodynamica: sive de viribus et motibus fluidorum commentarii.* Typographi Basiliensis; 1738.
14. Ye JB, Wang YT, Cai J, Chen QJ, He A. Influence of different combinations of impact mass and velocity with identical kinetic energy or momentum on the impact response of RC piles. *Mar Struct.* 2023;91:103462.